

AFFORD2ACT: Affordance-Guided Automatic Keypoint Selection for Generalizable and Lightweight Robotic Manipulation

Anukriti Singh¹, Kasra Torshizi¹, Khuzema Habib¹, Kelin Yu¹, Ruohan Gao¹, Pratap Tokekare¹

Abstract— Vision-based robot learning often relies on dense image or point-cloud inputs, which are computationally heavy and entangle irrelevant background features. Existing keypoint-based approaches can focus on manipulation-centric features and be lightweight, but either depend on manual heuristics or task-coupled selection, limiting scalability and semantic understanding. To address this, we propose AFFORD2ACT, an affordance-guided framework that distills a minimal set of semantic 2D keypoints from a text prompt and a single image. AFFORD2ACT follows a three-stage pipeline: affordance filtering, category-level keypoint construction, and transformer-based policy learning with embedded gating to reason about the most relevant keypoints, yielding a compact 38-dimensional state policy that can be trained in 15 minutes, which performs well in real-time without proprioception or dense representations. Across diverse real-world manipulation tasks, AFFORD2ACT consistently improves data efficiency, achieving an 82% success rate on unseen objects, novel categories, backgrounds, and distractors. Visualizations available at: <https://afford2act.github.io/>

I. INTRODUCTION

Learning effective robot manipulation policies hinges on overcoming a fundamental representation challenge: *how to extract the manipulation-related features which are both compact and expressive?* Dense visual inputs such as images [1], pointclouds [2], or semantic dense features [3], [4] provide rich details, but burden a policy with extraneous information. In contrast, 2D keypoint [5] offers a sparse state representation that highlights only the essential features of objects’ motions while still being representative enough to learn a good policy. This sparsity directly enables a lightweight policy with far fewer but important features than dense representation and support effective and real-time inference with less computational demand. However, the real challenge is in discovering these keypoints automatically and reliably: picking too few or irrelevant points can omit critical information, while relying on human insight for what points to use does not scale. In this paper, we present a method for identifying task-relevant object points that are both minimal (compact) and sufficient (expressive) for effective robot manipulation.

The problem of identifying keypoints has received a lot of attention recently. Some previous work utilizes manual selection [6] and prompts large Vision-Language Models (VLMs) to mark affordances on images [3], [7]. While these methods can provide useful cues, they depend on human guidance or external knowledge, making them labor-intensive and domain-specific. At the other end of the

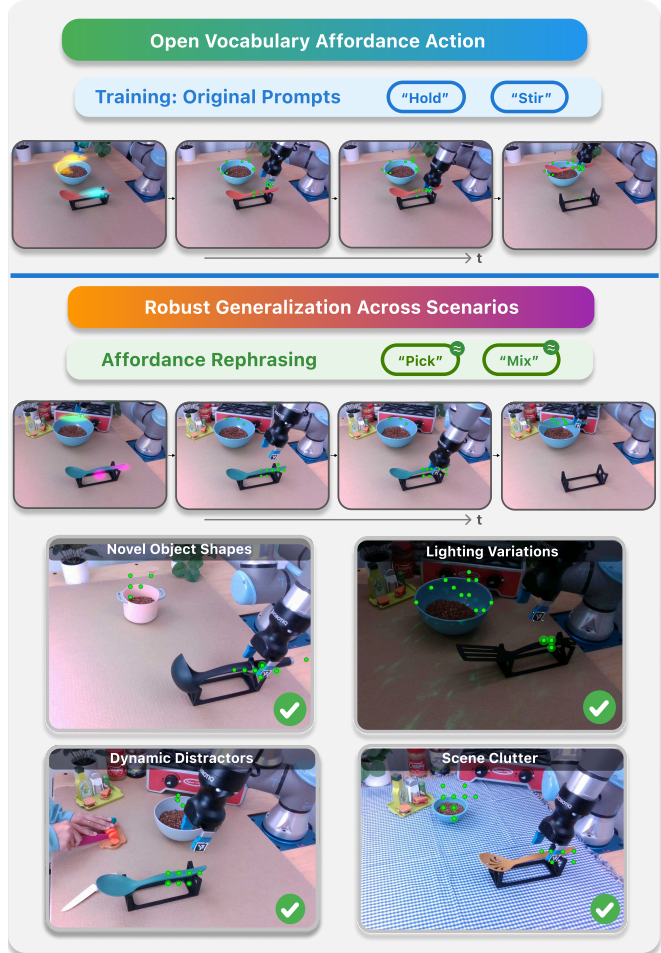


Fig. 1. **Top:** policy trained with original prompts (“hold”, “stir”) executes the actions over time (t). **Middle:** at test time, the same policy generalizes to synonym prompts (“pick”, “mix”). **Bottom:** affordance-guided keypoints with learned importance (green; variable count; ring radius \propto attention) remain stable under unseen object shapes, lighting conditions, dynamic distractors, and scene clutter—leading to successful rollouts.

spectrum, some approaches forgo sparsity altogether in favor of dense feature grid-based representations. For instance, all previous work [8]–[11] learn from dense grid of points in the scene or the object. While dense features are expressive, they are not compact and incur heavy computational demands. Furthermore, dense features may also entangle irrelevant dynamics (such as background features), which limits scalability and focus.

Recently, there has been work on automatically selecting a subset of keypoints from a dense grid [12]–[14] in an end-to-end manner. In particular, ATK [12] jointly optimizes a masking model for selecting a compact keypoint set and a task-specific control policy, yielding strong performance on

¹Department of Computer Science, University of Maryland, College Park, MD, USA. {anukriti, ktorsh, khabib, kyu85, rhgao, tokekare}@umd.edu

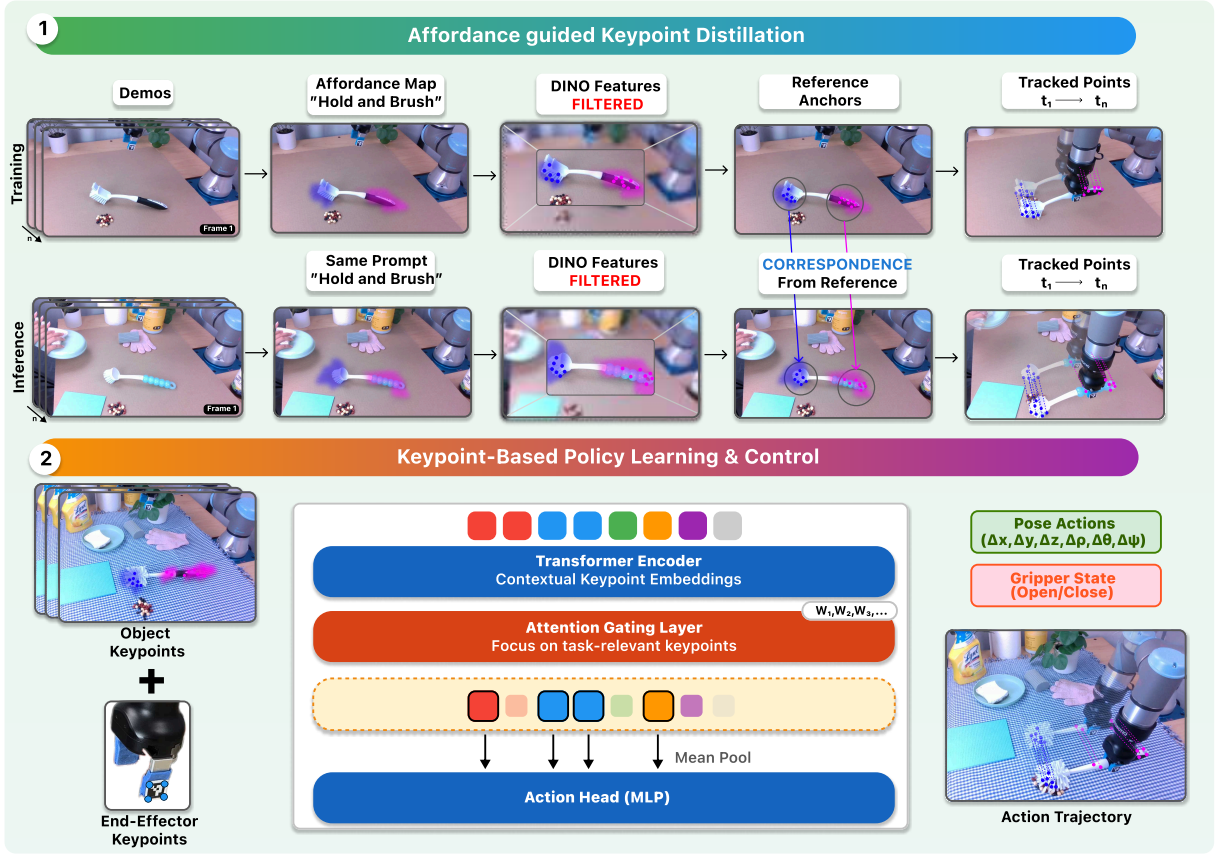


Fig. 2. **Overview of the AFFORD2ACT pipeline.** We extract task-relevant object keypoints using affordance masks and DINO filtering, track them across frames, and embed them with a transformer and attention gating. The policy head predicts pose and gripper commands from these compact keypoint representations, enabling vision-based manipulation without requiring proprioception.

challenging visuomotor tasks. However, there are two key limitations in ATK that prohibit it from generalizing: (i) Joint training couples the masking model to the task, so extending to a new task requires retraining both components (e.g., moving from mug picking from left to right); (ii) Existing evaluations emphasize robustness to positional variation and visual perturbations, whereas other generalization regimes, duplicate objects and cross-category transfer (e.g., from mugs to teapots), have received limited attention. In summary, prior works either require significant prior knowledge (manual keypoints), incur high computational overhead (dense grids), or struggle with stability and semantic generalization. This state of affairs motivates a core question for robot learning: *How can a robot learn to identify the most relevant interaction points, the task hotspots, directly from visual inputs?*

To address this challenge, we propose **AFFORD2ACT: Affordance-Guided Keypoints to Act**, which uses text-prompted affordance cues to automatically select task-relevant keypoints, with no manual labels. This pipeline contains three stages: (i) *Affordance Filtering* (e.g., “hold” → mug handle), (ii) *Keypoint Pool Construction* from a small set of masked DINO anchors, and (iii) *Keypoint-Based Policy Learning*, where a transformer-based encoder followed by a gating mechanism *learns the importance* of each keypoint. Because mask support and geometry vary, the number of selected keypoints per object also varies; thus, correspondence is defined as a flexible set of affordance-

region points. As visualized in Fig. 1, the policy typically attends to a small effective subset (Fig. 11) of keypoints. With a 38-dimensional input, policies remain robust under open-vocabulary prompts and scene changes across six real-world tasks. Evaluating across six real-world tasks, AFFORD2ACT consistently outperforms keypoint-selection baselines and RGB/RGB-D policies, and stays robust and generalizable to synonym prompts, lighting, distractors, and clutter (Fig. 1).

Contributions. We present:

- 1) A unified *Affordance-Guided Keypoint Distillation* framework that extracts sparse, semantically meaningful 2D keypoints directly from text prompts.
- 2) An efficient, attention-based framework that trains a compact keypoint-guided policy in ~ 15 minutes.
- 3) Extensive real-robot experiments in six tasks, demonstrating superior **82%** success in unseen instances and robustness to open-vocabulary prompts (Fig. 1).

II. RELATED WORK

Visual Representations for Policy Learning: Choosing the right visual representation is central to building robust manipulation policies. Classic approaches rely on raw sensory data which includes images, depth maps, or point clouds to provide a complete view of the environment [1], [2], [15]. While these representations are rich, they also saddle policies with high-dimensional inputs, requiring heavy data regimes and often resulting in policies that overfit to appearance

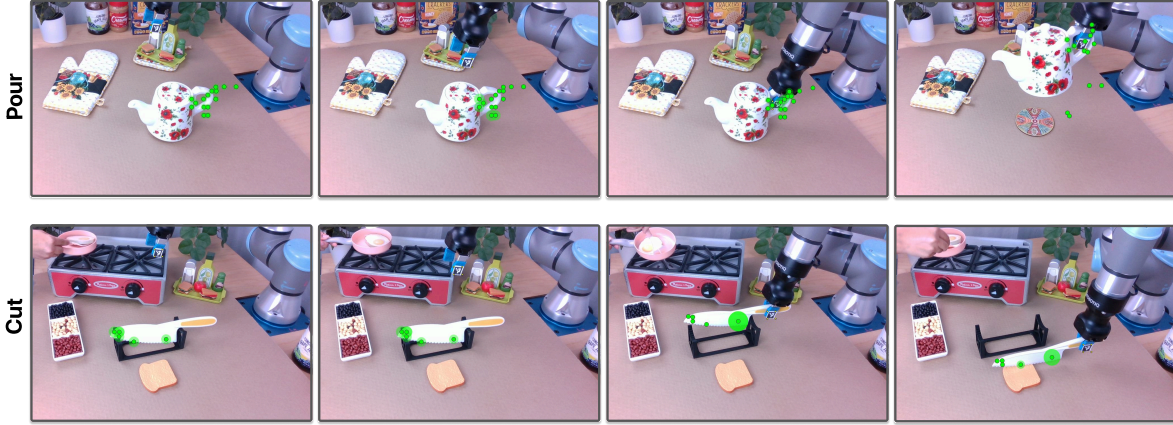


Fig. 3. Real-world rollouts of AFFORD2ACT on Pour (top) and Cut (bottom) tasks. In each sequence (left to right: approach → interaction → completion), green dots mark keypoints automatically selected on the affordance region (e.g., knife for “cut”, handle/spout for “pour”). The translucent ring size reflects the attention weight at each step. While keypoints remain fixed on task-relevant parts, the policy dynamically shifts its focus: for “cut”, the attention moves from the blade tip toward the handle; for “pour”, from the edge to the main handle. This adaptive attention enables robust, context-aware manipulation.

rather than task. As a remedy, manipulation-centric and object-centric representations [3], [16]–[21] filter out much of the visual clutter, focusing policy learning on the handful of features that matter most for action. However, these strategies often rely on hand-tuned detectors or dense input from images 3D reconstructions, limiting scalability and flexibility. Our method bypasses these constraints, extracting a compact, affordance-driven set of 2D keypoints that serve as a focused visual state, requiring neither dense geometry nor extensive supervision.

Keypoints and Automatic Anchor Discovery: Keypoints, when properly chosen, offer a natural low-dimensional representation that encodes an object’s essential affordances [6], [10], [11], [14]. Earlier work often assumed keypoints could be specified by experts, or required laborious labeling to maintain semantic consistency across objects [6], [22]. More recent efforts automate this selection, using object detector [10], [11] or learning which points are most predictive for the task at hand [8], [12]. For keypoint sampling from detected objects, the representations are still dense and lack semantic meaning. ATK, for instance, integrates keypoint selection with policy optimization, but can produce unstable and semantically ambiguous anchors. VLM-driven pipelines like MOKA [7] bring zero-shot power to keypoint discovery, but still rely on iterative visual prompting or domain knowledge. Our approach sidesteps both manual bias and unstable end-to-end discovery by using affordance cues as a reliable guide, automatically surfacing keypoints that are functionally meaningful and consistent, without relying on heavy annotation or black-box prompts.

Affordance Reasoning in Manipulation: The concept of affordances has become foundational in robotics, bridging perception and action by focusing on what an object “invites” a robot to do [23], [24]. Early works constructed dense affordance maps [25]–[27] or trained region classifiers, but these methods faced challenges in scaling and generalization. The rise of vision-language models and foundation models [7], [28] brought a new wave of affordance reasoning, inferring actionable regions from text and image cues. However,

the leap from model outputs to actionable robot inputs is nontrivial: such approaches can be coarse, ambiguous, or computationally heavy. In contrast, we use affordance signals to guide the distillation of sparse, actionable keypoints, ensuring the resulting representation is both semantically grounded and directly useful for policy learning, combining the semantic strengths of foundation models with the simplicity and efficiency of classic keypoint methods.

III. AFFORD2ACT

Overview. Given single-view demonstrations $\mathcal{D} = \{(I_{1:T_d}^{(d)}, \mathbf{u}_{1:T_d}^{(d)}, A^{(d)})\}_{d=1}^D$, where $I_t^{(d)} \in \mathbb{R}^{H \times W \times 3}$ are images, $\mathbf{u}_t^{(d)} \in \mathbb{R}^m$ are actions (e.g., 6-DoF deltas and a gripper scalar), and $A^{(d)}$ is a text prompt, AFFORD2ACT: (i) localizes the actionable region via a prompt-conditioned affordance mask (Section III-A), (ii) selects a small set of semantic keypoints on the reference frame (Section III-A), (iii) matches them *within the mask* on new instances to establish flexible correspondence (≤ 15) for various geometry and lighting (Section III-A), (iv) jointly tracks selected keypoints and encodes them into a transformer with a gating layer that *learns phase-adaptive weights* to encode a compact scene embedding for policy learning (Section III-B). The overall framework is shown in Fig. 2.

Formal Setup. Each demonstration d is summarized by trajectories of K 2D keypoints $\mathbf{P}^{(d)} = \{(x_{t,i}^{(d)}, y_{t,i}^{(d)})\}_{t=1:T_d, i=1:K}$, where indices i refer to functional parts within the affordance region (e.g., “handle tip,” “blade edge”). This sparse, semantic representation lets the policy reason over roles rather than raw pixels.

A. Affordance-Guided Keypoint Representation

Our pipeline for extracting these keypoints proceeds in four stages, all fully automatic and requiring no manual annotation (See Fig. 2).

Affordance Localization: Given the first frame I_1 of a demonstration affordance prompt, we use One-Shot Open Affordance model [28] f_{aff} to produce a heatmap: $H = f_{\text{aff}}(I_1, A) \in [0, 1]^{H \times W}$. This heatmap indicates regions of the scene that likely correspond to the intended action. To

focus only on the actionable surface, we apply a robust quantile threshold (along with mild smoothing) to obtain a binary mask: $M(x, y) = \mathbb{1}[H(x, y) \geq \tau_q(H)]$. This mask captures fine structures such as a knife blade or cup rim and robustly filters out clutter. Text-based prompts provide a strong semantic prior, allowing the same model to adapt affordance detection across novel tools or object categories with minimal (such as the examples in Fig. 3).

Reference Keypoint Extraction: On a reference frame (in our case, the first frame of the first demonstration), I_1^r , we compute dense feature maps using a Vision Transformer backbone (ViT/DINO) [29]: $F_r = \phi(I_1^r) \in \mathbb{R}^{H \times W \times D}$. We then restrict attention to the ROI defined by the affordance mask M and cluster the features within that region to obtain N reference anchor points:

$$\mathcal{A}_r = \{(p_i^r, \mathbf{f}_i^r)\}_{i=1}^N, \quad p_i^r \in \Omega(M), \quad \mathbf{f}_i^r = F_r(p_i^r)$$

This step is fully automatic and scales to new categories, in contrast to manual annotation-based approaches [6], [7].

Cross-instance Correspondence: Given a new demonstration, we extract features from its first frame, $F_t = \phi(I_1^t)$. From each keypoint, (p_i^r, \mathbf{f}_i^r) in the reference anchor, \mathcal{A}_r , we compute a cosine similarity map restricted to the affordance ROI in the new frame:

$$S_i(x, y) = \left\langle \frac{\mathbf{f}_i^r}{\|\mathbf{f}_i^r\|}, \frac{F_t(x, y)}{\|F_t(x, y)\|} \right\rangle, \quad (x, y) \in \Omega(M_t)$$

We assign the keypoint with the highest similarity,

$$p_i^t = \arg \max_{(x, y) \in \Omega(M_t)} S_i(x, y), \quad c_i^t = \max_{(x, y) \in \Omega(M_t)} S_i(x, y)$$

This matching ensures that the index i refers to the same functional part (e.g., “handle tip”) across all demonstrations, even as object geometry and appearance vary. By constraining matches to the affordance mask, we avoid drifting to irrelevant but visually similar regions.

Temporal Keypoint Tracking: Once all K keypoints are initialized on the first frame, we track them across the demonstration using a transformer-based tracker such as CoTracker [30]: $\{p_{t,i}\}_{t=1:T, i=1:K} = g_{\text{trk}}(I_{1:T}, \{p_i^1\}_{i=1}^K)$

Joint tracking improves robustness to occlusion and viewpoint changes, leveraging correlations among keypoints. The output is a set of trajectories in a semantic space where each index i always refers to the same actionable region.

By the end of this process, every demonstration is described by a trajectory of K task-relevant, affordance-grounded keypoints. This sparse and semantically aligned representation serves as the input to our downstream policy (Section III-B), bridging the gap between the efficiency of keypoints and the semantic expressiveness of affordances, without requiring heavy 3D pipelines or manual keypoint curation.

B. Policy Design

At each interfere step t , taking the K keypoints from keypoint distillation $\{p_{t,i}\}_{i=1}^K$, the question becomes: *how do we architect a policy, π_θ , that prioritizes the most task-relevant keypoints?* After embedding each keypoint, $z^1 = [\phi_\theta(p_1) \dots \phi_\theta(p_K)]^\top$, we then compute *contextualized token*



Fig. 4. (Left) A figure of our physical setup, composing of a UR3e Robotic arm and one side RealSenseD435i Camera. (Right) shows the objects we used for seen (right) and unseen (left) scenarios.

features using a Transformer chunk, $z = \mathcal{T}_\theta(z_1)$, similar to [31], [32] so that each keypoint is interpreted in the context of the others (e.g., a keypoint on the blade of a knife carries a different affordance than one on the handle). Since the number of keypoints m can exceed the task-relevant cardinality, we introduce a **gating network**, g_ψ , that predicts a non-negative importance weight for each keypoint before pooling them into a single scene feature vector h :

$$\hat{w} = g_\psi(z) = \text{softmax}(w_g^\top z + b_g), \quad \hat{z} = \hat{w}^\top z, \quad h = \frac{1}{K} \sum_{i=1}^K \hat{z}_i$$

Then, the scene embedding, h is passed through a shared action head that is later split into two linear layers: one for the delta actions and the other for the gripper state. While we use a two-layer MLP, the head is modular and can be replaced by a generative policy head [1], [33], [34].

IV. EXPERIMENTS

Our experiments are designed to evaluate three claims:

- 1) **Keypoint Effectiveness:** Can a policy trained exclusively on a compact set of 2D keypoints outperform policies trained on full images, dense features, and even a large vision-language foundation model?
- 2) **Keypoint Priors:** Which alternative keypoint selection strategies (e.g., using object bounding box, uniform grids of points, or manually selected points) can match the informativeness of our affordance-guided keypoints?
- 3) **Generalization:** How well does our policy generalize to new scenarios, including novel objects within seen categories, entirely new object categories, the presence of distractor objects, and other scene variations?

Additionally, we perform targeted ablation studies to test the robustness to different language prompts, to verify the necessity of the gating network, and to explore an extended two-stage pipeline for long-horizon tasks.

A. Setup and Tasks

Our method is driven by task semantics expressed as natural-language prompts that condition an affordance model. We focus on these core affordances—*hold*, *cut_with*, *brush_with*, *pour*, and *kick*—and systematically construct a variety of manipulation tasks by pairing each affordance with diverse objects and contexts. The mapping from affordances to example tasks is as follows:

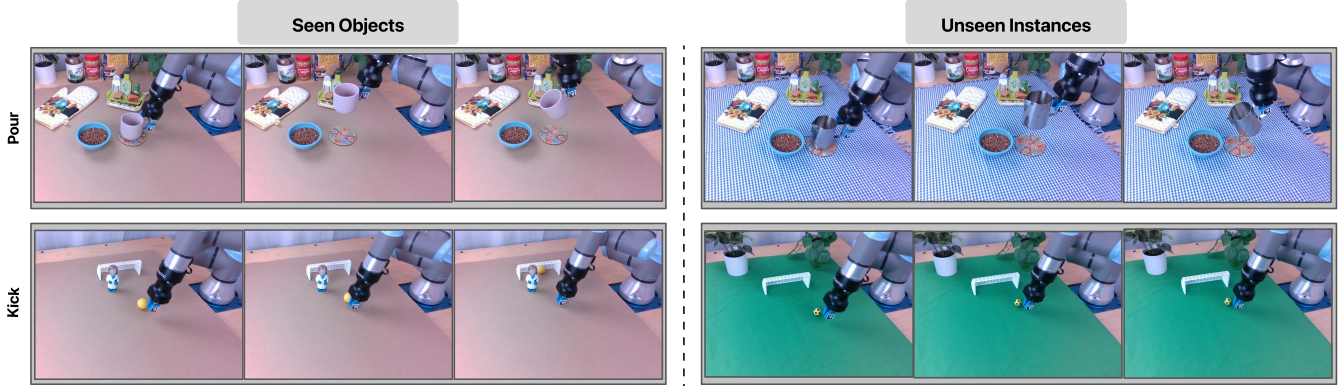


Fig. 5. **Qualitative generalization on two tasks.** Each row shows rollouts for *Pour* (top) and *Kick* (bottom). **Left:** training objects (seen). **Right:** held-out settings with unseen scenes (new backgrounds/tabletops) and, for *Pour*, unseen object instances. Within each panel we show three key frames (setup, approach, completion). Without any test-time adaptation, AFFORD2ACT trained from single-view RGB using affordance-guided keypoints successfully transfers by attending to the functional part (mug handle / ball) while ignoring clutter.

Hold: Grasp and lift an object with a handle (e.g., a mug) using the *hold* affordance. (Fig. 1)

Cut: Perform a cutting motion on an object using a knife, guided by the *cut_with* affordance. (Fig. 3)

Brush: Sweep debris using a hand brush. This task leverages both the *hold* and *brush_with* affordances in coordination (holding the brush and using it to brush). (Fig. 2)

Pour: Execute a pouring motion with a vessel (e.g., tipping a cup or pitcher) using the *pour* affordance. (Fig. 5)

Stir: Stir the contents of a bowl using a spoon or similar tool, guided by a combination of *hold* (to grasp the spoon) and a *stir* affordance. (Fig. 1)

Kick: Push a ball into a goal using the *kick* affordance. 5

For each task, we train a policy and test it with a variety of seen and novel objects (see Fig. 4). The objects are physically diverse in size, shape, appearance, and material. This diversity allows us to evaluate generalization at both the instance level (new objects of a trained category) and the category level (objects from entirely new categories). We collected 40 teleoperated demonstrations per task for training, with object positions randomized across demonstrations.

B. Input Modality Baselines

We benchmark our approach against four baseline methods to evaluate the keypoints effectiveness:

- **RGB-BC:** A behavior cloning policy trained on raw RGB images, using a ResNet-18 visual encoder and a multilayer perceptron (MLP) for the action output.
- **RGB-D-BC:** The framework as RGB-BC, but trained on 4-channel RGB-D images (RGB plus monocular depth from an Intel RealSense camera).
- **UAD-2D-BC:** The same framework as RGB-BC, but the images are replaced with the affordance mask generated by UAD [3]. This baseline can verify the effectiveness of sparse keypoints rather than dense representations.
- **Foundation Model (Pi0):** A large vision-language-action foundation model (Pi0) [35] fine-tuned on our demonstration data. We evaluate this model with a single side camera on a UR3e robot arm, which are settings that Pi0 has not encountered during its training.

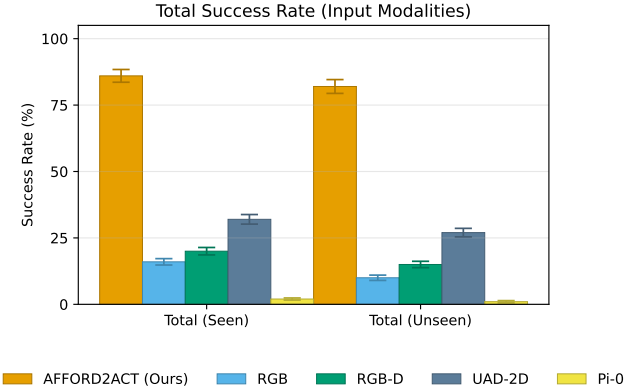


Fig. 6. Total Average success rate across input modalities. For each input modality, we test on 20 trials on each task, then average the results. We split the success rates of seen and unseen instances (detailed in Section IV-E).

C. Evaluation Protocol and Metrics

Success Rate: We evaluate each policy on 20 real-world episodes per task and report per-task success split by *seen* vs. *unseen* instances (Fig. 6). Our keypoint-based policy consistently outperforms RGB and RGB-D baselines, especially on unseen objects—likely because dense RGB inputs overfit to a single environment. For the UAD baseline, although it can extract dense features from the objects, it fails short with small number of demonstration because of its high-dimension representations. In contrast, the Pi0 foundation model struggled on most tasks. The first reason is that our setup uses only an external camera view, whereas Pi0 was designed to also use a wrist-mounted camera. Secondly, Pi0’s underlying vision-language model (PaLI-GEMMA) is relatively small, which required more data to refine and also made it sensitive to the language instructions.

Semantic Trajectory Metrics: To diagnose failures beyond binary task success, we create a rubric to score each trajectory (as suggested by [36]). The rubric breaks captures the success of several intermediate steps and not just the final task success (Fig. 7). In our evaluation, each sub-goal is checked independently, meaning we record whether the policy managed to achieve each individual step. To this end, we found cases where the RGB and RGB-D BC policies

Sub-goal	Ours (Y/N)	RGB (Y/N)	RGB-D (Y/N)	Pi-0 (Y/N)	UAD-2D (Y/N)
Overall success?	43/7	8/42	10/40	2/48	16/34
Aligned with object?	47/3	26/24	31/9	6/44	36/14
Grasped object?	44/6	12/38	21/29	3/47	26/24
Completed final motion?	43/7	16/34	14/36	2/48	19/31
Robot collided?	1/49	10/40	6/44	46/4	6/44

Fig. 7. Semantic Information rubric scores across input modalities on seen instances. For each input modality, we collected 40 trials for each task (we exclude the ball kick task as there is no notion of grasping). The success/failed shown as Y/N in the table for each sub-goal are manually recorded.

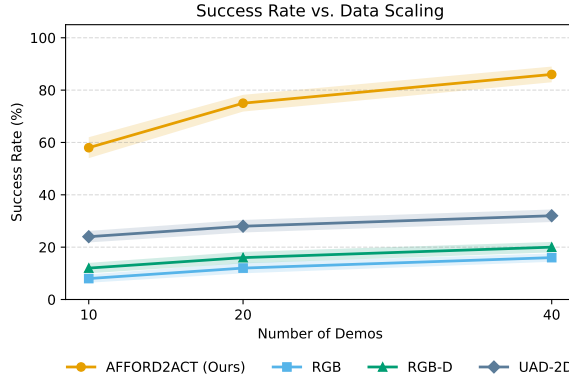


Fig. 8. AFFORD2ACT outperforms all baselines even with just 10 demonstrations, with the performance gap remaining consistent as more demos are added. Standard deviation bars show variability across tasks.

attempted to perform the final motion of the task (such as pouring or cutting) before actually grasping the object, indicating a confusion in the sequence of actions. In contrast, our keypoint-based policy typically reaches the final sub-goal, with occasional last-step slippage (object slipping from the gripper), suggesting strong early-stage competence.

Data Scaling: We study the effect of demonstration data size by training each method on progressively smaller subsets of the data. In particular, we downsampled the demonstrations to 50% and 25% of the full set and measured the success rates (Fig. 8). The results show that our keypoint-based method remains highly effective even with far fewer demonstrations, whereas the image-based baselines degrade significantly as the training data is reduced. This highlights the data efficiency of our approach compared to learning directly from raw images.

D. Keypoints Selections Baselines

After demonstrating that a 2D keypoint-based policy can be highly effective, we ask whether our affordance-driven keypoint selection is essential. We compare our approach with several alternative keypoint selection strategies, each using $K = 19$ (15 on object and 4 on end-effector) keypoints and the same downstream policy architecture for fairness:

YOLO [37] + DINO [29]: Use a YOLO object detector to generate bounding boxes, then sample DINO keypoint correspondences within each detected box.

YOLO [37] + Uniform Grid: Uniformly sample a grid of points inside each YOLO-detected bounding box.

DINO [29] Only: Use DINO to generate correspondences over the entire image without bounding-box or filtering.

SAM [38] + DINO: Use the Segment Anything Model (SAM) to obtain segmentation masks, use YOLO to identify the target object’s mask, and then sample DINO correspondences within that segmented region.

Hand-Picked (P3PO): An oracle baseline where an expert manually chooses the keypoints (following P3PO [6]), and these points are then tracked using DIFT + CoTracker.

Fig. 9 summarizes the success rates of these strategies, averaged across all tasks, for both seen and unseen object instances. We find that the methods relying on YOLO detection do not significantly improve generalization to unseen object categories. This is likely because they depend on known object class labels (e.g., always looking for a “cup”), which can be misguiding when the object geometry changes (for example, encountering a teapot that might not be recognized as a cup). It also can suffer in cluttered scenes when the boxes are not tight or when multiple objects are present. In contrast, our affordance-driven approach does not depend on specific object labels; it directly identifies task-relevant regions (interaction hotspots) via the affordance model. We also note that the manually selected keypoints (P3PO) yield a success rate nearly on par with AFFORD2ACT. However, our method achieves this performance without the tedious manual effort of choosing points, and it offers the flexibility of using natural language to specify the task.

E. Generalization Analysis

Beyond evaluating overall success, we systematically test four axes of generalization to assess how well AFFORD2ACT transfers to new situations:

- 1. Unseen Object (Same Category):** Test the policy on novel instances of the same category (e.g., a new mug for the “hold” task or a different brush for “brush_with”).
- 2. Unseen Category:** Apply the learned skill to an object from a category not encountered during training (e.g., using a spatula to stir instead of a spoon).
- 3. Background Variation:** Evaluate the policy in environments with different backgrounds or lighting conditions.
- 4. Distractors:** Introduce additional objects or even moving agents (e.g., a person performing an unrelated action nearby) to test the policy’s ability to stay focused on the target task in the presence of distractions.

Fig. 10 illustrates these generalization scenarios and the corresponding performance. Our keypoint-based policy exhibits strong transferability to novel object instances within seen categories and even to objects from entirely new categories (essentially achieving zero-shot generalization). It also remains robust under background changes and in cluttered environments. For example, in one challenging trial, the system successfully transferred the learned affordance to a teapot from a mug in a highly cluttered scene, correctly identifying the meaningful keypoints despite different geometry. Likewise, the policy proved resilient to dynamic distractions, even with a human actively moving nearby.

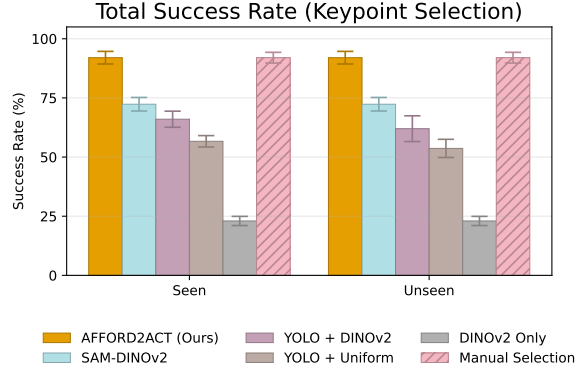


Fig. 9. Total Average success rate across keypoint selection methods.

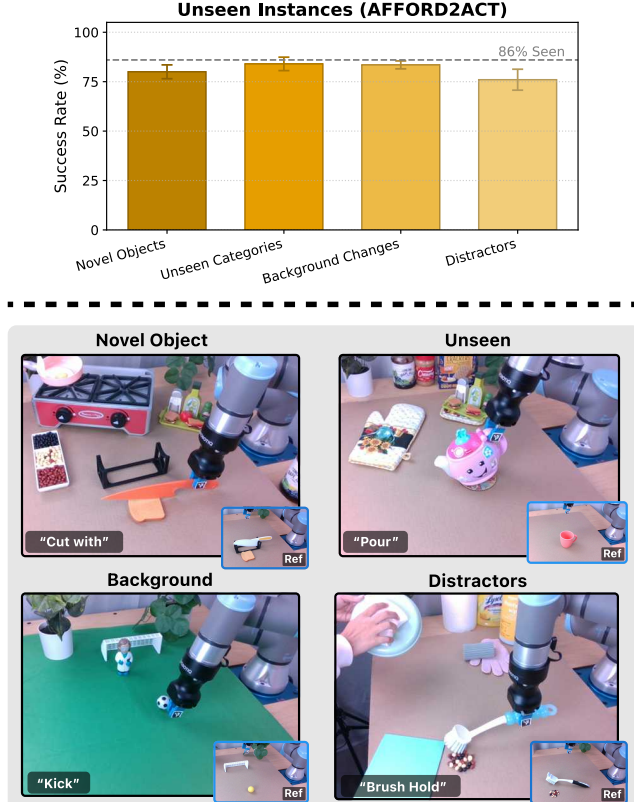


Fig. 10. **Top:** Average success rate on four scenarios aggregated across all tasks. **Bottom:** Representative rollouts for each scenario. The small inset labeled “Ref” shows the training reference object for that task.

F. Ablation Studies

We conducted additional ablations to highlight the contribution of different components of our pipeline:

Language Prompt Robustness: We varied the wording of the affordance prompt to ensure our approach is not overly sensitive to specific language. Qualitatively, we found that synonyms or related phrases produce similar affordance key-points. For example, using “sweep” instead of “brush_with” or “pick_up” instead of “hold” resulted in nearly identical affordance predictions on the relevant objects, indicating the model robustly understands the intended action.

Gating Network: We removed the gating network so that each keypoint token receives equal weighting. This modification significantly degraded performance (especially

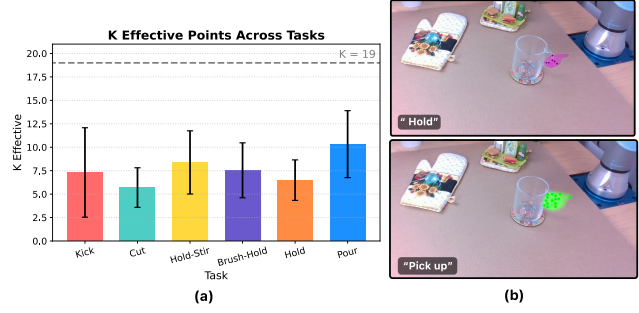


Fig. 11. Average effective number of keypoints used (over all time steps) for each task. This data was collected through offline inference on all 40 training demos for each task.

in cluttered scenes), reducing the overall success rate from 86% to 52%. During trajectory rollout, the gating mechanism allows the policy to focus only on the keypoints necessary.

Effective Keypoint Count: We analyzed the gating network’s behavior by computing the effective number of keypoints being used by the policy at each time step. Given the gating output weights w_i for the K keypoint tokens, we define $K_{\text{eff}} = 1 / \sum_{i=1}^K w_i^2$. In our experiments, K_{eff} was typically much smaller than the total number of points $K = 19$, as shown in Fig. 11. This implies that the gating network effectively attends to only a subset of the keypoints at any given time, which helps the policy concentrate on the most informative features for the task.

G. Long-Horizon Skills via Two-Stage Re-Anchoring

For more complex, multi-phase tasks, we integrate Large Model task planning stage into our framework. We first use a vision-language model (VLM) planner to detect when the first sub-goal of the task has been completed (e.g., when the robot has successfully grasped the object). Once this condition is detected, we re-anchor half of the keypoints by providing an updated affordance prompt for the next phase of the task. In practice, this means replacing roughly half of the original keypoints with new ones tailored to the subsequent sub-task. This re-anchoring allows the policy to adapt to the changed state of the scene and effectively execute the next stage in the trajectory. We experimented with this augmentation on the *Stir* task, achieving an impressive 90% success rate, further showing promise with incorporating VLMs with affordance-based keypoint selection (see video).

V. CONCLUSIONS AND FUTURE WORK

We introduced **AFFORD2ACT**, a three-stage imitation learning pipeline that leverages semantically meaningful keypoints derived from affordance text prompts. Through six real-world experiments, we demonstrated that AFFORD2ACT is not only data-efficient and performant, but also generalizes effectively to unseen objects, categories, backgrounds, and distractors. While our work represents the first attempt at semantically meaningful keypoint-based imitation learning, the selected keypoints remain fixed during inference and cannot be adapted dynamically to evolving contexts. As

discussed in Sec. IV-G, integrating task planning with key-point resampling is a promising future direction, potentially enabling flexible long-horizon policy execution.

REFERENCES

- [1] C. Chi, Z. Xu, C. Pan, E. Cousineau, B. Burchfiel, S. Feng, R. Tedrake, and S. Song, “Diffusion policy: Visuomotor policy learning via action diffusion,” *The International Journal of Robotics Research*, 2024, journal version; earlier preprint available on arXiv.
- [2] Y. Ze, G. Zhang, K. Zhang, C. Hu, M. Wang, and H. Xu, “3d diffusion policy: Generalizable visuomotor policy learning via simple 3d representations,” 2024. [Online]. Available: <https://arxiv.org/abs/2403.03954>
- [3] Y. Tang, W. Huang, Y. Wang, C. Li, R. Yuan, R. Zhang, J. Wu, and L. Fei-Fei, “Uad: Unsupervised affordance distillation for generalization in robotic manipulation,” 2025. [Online]. Available: <https://arxiv.org/abs/2506.09284>
- [4] Y. Wang, G. Yin, B. Huang, T. Kelestemur, J. Wang, and Y. Li, “Gendp: 3d semantic fields for category-level generalizable diffusion policy,” 2024. [Online]. Available: <https://arxiv.org/abs/2410.17488>
- [5] C. Doersch, Y. Yang, M. Vecerik, D. Gokay, A. Gupta, Y. Aytar, J. Carreira, and A. Zisserman, “Tapir: Tracking any point with per-frame initialization and temporal refinement,” in *Proceedings of the IEEE/CVF International Conference on Computer Vision*, 2023, pp. 10061–10 072.
- [6] M. Levy, S. Haldar, L. Pinto, and A. Shirivastava, “P3-po: Prescriptive point priors for visuo-spatial generalization of robot policies,” 2024. [Online]. Available: <https://arxiv.org/abs/2412.06784>
- [7] F. Liu, K. Fang, P. Abbeel, and S. Levine, “MOKA: Open-vocabulary robotic manipulation through mark-based visual prompting,” in *First Workshop on Vision-Language Models for Navigation and Manipulation at ICRA 2024*, 2024. [Online]. Available: <https://openreview.net/forum?id=K8eoYUofbQ>
- [8] C. Wen, X. Lin, J. So, K. Chen, Q. Dou, Y. Gao, and P. Abbeel, “Any-point trajectory modeling for policy learning,” 2024. [Online]. Available: <https://arxiv.org/abs/2401.00025>
- [9] H. Bharadhwaj, R. Mottaghi, A. Gupta, and S. Tulsiani, “Track2act: Predicting point tracks from internet videos enables generalizable robot manipulation,” 2024. [Online]. Available: <https://arxiv.org/abs/2405.01527>
- [10] M. Xu, Z. Xu, Y. Xu, C. Chi, G. Wetzstein, M. Veloso, and S. Song, “Flow as the cross-domain manipulation interface,” 2024. [Online]. Available: <https://arxiv.org/abs/2407.15208>
- [11] K. Yu*, S. Zhang*, H. Soora, F. Huang, H. Huang, P. Tokekar, and R. Gao, “Genflowrl: Shaping rewards with generative object-centric flow in visual reinforcement learning,” in *International Conference on Computer Vision (ICCV)*, 2025.
- [12] Y. Zhang, S. Mittal, Z. Zhang, L. Ke, S. Srinivasa, and A. Gupta, “Atk: Automatic task-driven keypoint selection for robust policy learning,” 2025. [Online]. Available: <https://arxiv.org/abs/2506.13867>
- [13] J. Gao, Z. Tao, N. Jaquier, and T. Asfour, “K-vil: Keypoint-based visual imitation learning,” *IEEE Transactions on Robotics*, vol. 39, no. 5, p. 3888–3908, Oct. 2023. [Online]. Available: <http://dx.doi.org/10.1109/TRO.2023.3286074>
- [14] S. Wang, J. You, Y. Hu, J. Li, and Y. Gao, “Skil: Semantic keypoint imitation learning for generalizable data-efficient manipulation,” in *Proceedings of Robotics: Science and Systems (RSS)*, 2025. [Online]. Available: <https://www.roboticsproceedings.org/rss21/p161.pdf>
- [15] A. Zeng, S. Song, K.-T. Yu, E. Donlon, F. Hogan, M. Bauza, D. Ma, O. Taylor, M. Liu, E. Romo, N. Fazeli, F. Alet, P. Isola, A. Torralba, A. Rodriguez, L. P. Kaelbling, and T. Lozano-Pérez, “Robotic pick-and-place of novel objects in clutter with multi-affordance grasping and cross-domain image matching,” in *2018 IEEE International Conference on Robotics and Automation (ICRA)*. IEEE, 2018, pp. 3750–3757.
- [16] E. Jang, S. Vijayanarasimhan, P. Pastor, J. Ibarz, and S. Levine, “End-to-end learning of semantic grasping,” in *Proceedings of the 1st Annual Conference on Robot Learning*, ser. Proceedings of Machine Learning Research, S. Levine, V. Vanhoucke, and K. Goldberg, Eds., vol. 78. PMLR, 13–15 Nov 2017, pp. 119–132. [Online]. Available: <https://proceedings.mlr.press/v78/jang17a.html>
- [17] P. R. Florence, L. Manuelli, and R. Tedrake, “Dense object nets: Learning dense visual object descriptors by and for robotic manipulation,” in *Proceedings of The 2nd Conference on Robot Learning*, ser. Proceedings of Machine Learning Research, A. Billard, A. Dragan, J. Peters, and J. Morimoto, Eds., vol. 87. PMLR, 29–31 Oct 2018, pp. 373–385. [Online]. Available: <https://proceedings.mlr.press/v87/florence18a.html>
- [18] M. Shridhar, L. Manuelli, and D. Fox, “Perceiver-actor: A multi-task transformer for robotic manipulation,” in *Proceedings of The 6th Conference on Robot Learning*, ser. Proceedings of Machine Learning Research, K. Liu, D. Kulic, and J. Ichniowski, Eds., vol. 205. PMLR, 14–18 Dec 2023, pp. 785–799. [Online]. Available: <https://proceedings.mlr.press/v205/shridhar23a.html>
- [19] P. Yu, A. Bhaskar, A. Singh, Z. Mohammad, and P. Tokekar, “Sketch-to-skill: Bootstrapping robot learning with human drawn trajectory sketches,” 2025. [Online]. Available: <https://arxiv.org/abs/2503.11918>
- [20] W. Tang, J.-H. Pan, W. Zhan, J. Zhou, H. Yao, Y.-H. Liu, M. Tomizuka, M. Ding, and C.-W. Fu, “Embodiment-agnostic action planning via object-part scene flow,” 2024. [Online]. Available: <https://arxiv.org/abs/2409.10032>
- [21] C.-C. Hsu, B. Wen, J. Xu, Y. Narang, X. Wang, Y. Zhu, J. Biswas, and S. Birchfield, “Spot: Se(3) pose trajectory diffusion for object-centric manipulation,” 2025. [Online]. Available: <https://arxiv.org/abs/2411.00965>
- [22] L. Manuelli, W. Gao, P. Florence, and R. Tedrake, “kpam: Keypoint affordances for category-level robotic manipulation,” 2019. [Online]. Available: <https://arxiv.org/abs/1903.06684>
- [23] J. J. Gibson, *The Ecological Approach to Visual Perception*. Hillsdale, NJ: Lawrence Erlbaum Associates, 1979.
- [24] M. Ciocarlie, C. Goldfeder, and P. K. Allen, “Dimensionality reduction for hand-independent dexterous robotic grasping,” *The International Journal of Robotics Research*, vol. 28, no. 7, pp. 851–871, 2009.
- [25] A. Myers, C. L. Teo, C. Fermüller, and Y. Aloimonos, “Affordance detection of tool parts from geometric features,” in *IEEE International Conference on Robotics and Automation (ICRA)*, 2015, pp. 1374–1381.
- [26] T.-T. Do, A. Nguyen, and I. Reid, “Affordancenet: An end-to-end deep learning approach for object affordance detection,” in *IEEE International Conference on Robotics and Automation (ICRA)*, 2018.
- [27] S. Bahl, R. Mendonca, L. Chen, U. Jain, and D. Pathak, “Affordances from human videos as a versatile representation for robotics,” *CVPR*, 2023.
- [28] G. Li, D. Sun, L. Sevilla-Lara, and V. Jampani, “One-shot open affordance learning with foundation models,” in *Proceedings of the IEEE/CVF Conference on Computer Vision and Pattern Recognition (CVPR)*, 2024.
- [29] M. Oquab, T. Darcret, T. Moutakanni, H. V. Vo, M. Szafraniec, V. Khalidov, P. Fernandez, D. HAZIZA, F. Massa, A. El-Nouby, M. Assran, N. Ballas, W. Galuba, R. Howes, P.-Y. Huang, S.-W. Li, I. Misra, M. Rabbat, V. Sharma, G. Synnaeve, H. Xu, H. Jegou, J. Mairal, P. Labatut, A. Joulin, and P. Bojanowski, “DINOv2: Learning robust visual features without supervision,” *Transactions on Machine Learning Research*, 2024, featured Certification. [Online]. Available: <https://openreview.net/forum?id=a68SUt6zFt>
- [30] N. Karaev, I. Rocco, B. Graham, N. Neverova, A. Vedaldi, and C. Rupprecht, “Cotracker: It is better to track together,” in *European conference on computer vision*. Springer, 2024, pp. 18–35.
- [31] S. Haldar, Z. Peng, and L. Pinto, “Baku: An efficient transformer for multi-task policy learning,” 2024. [Online]. Available: <https://arxiv.org/abs/2406.07539>
- [32] T. Z. Zhao, V. Kumar, S. Levine, and C. Finn, “Learning fine-grained bimanual manipulation with low-cost hardware,” 2023. [Online]. Available: <https://arxiv.org/abs/2304.13705>
- [33] C. Lynch, M. Khansari, T. Xiao, V. Kumar, J. Tompson, S. Levine, and P. Sermanet, “Learning latent plans from play,” 2019. [Online]. Available: <https://arxiv.org/abs/1903.01973>
- [34] N. M. M. Shafullah, Z. J. Cui, A. Altanzaya, and L. Pinto, “Behavior transformers: Cloning k modes with one stone,” 2022. [Online]. Available: <https://arxiv.org/abs/2206.11251>
- [35] K. Black, N. Brown, D. Driess, A. Esmail, M. Equi, C. Finn, N. Fusai, L. Groom, K. Hausman, B. Ichter, S. Jakubczak, T. Jones, L. Ke, S. Levine, A. Li-Bell, M. Mothukuri, S. Nair, K. Pertsch, L. X. Shi, J. Tanner, Q. Vuong, A. Walling, H. Wang, and U. Zhilinsky, “ π_0 : A vision-language-action flow model for general robot control,” 2024. [Online]. Available: <https://arxiv.org/abs/2410.24164>

- [36] H. Kress-Gazit, K. Hashimoto, N. Kuppuswamy, P. Shah, P. Horgan, G. Richardson, S. Feng, and B. Burchfiel, “Robot learning as an empirical science: Best practices for policy evaluation,” *arXiv preprint arXiv:2409.09491*, 2024.
- [37] J. Redmon, S. Divvala, R. Girshick, and A. Farhadi, “You only look once: Unified, real-time object detection,” 2016. [Online]. Available: <https://arxiv.org/abs/1506.02640>
- [38] A. Kirillov, E. Mintun, N. Ravi, H. Mao, C. Rolland, L. Gustafson, T. Xiao, S. Whitehead, A. C. Berg, W.-Y. Lo, P. Dollár, and R. Girshick, “Segment anything,” 2023. [Online]. Available: <https://arxiv.org/abs/2304.02643>